Exploratory investigation on mechanical anchors for connecting SMA bars to steel or FRP bars

M. Shahria Alam[1], Maged A. Youssef[2] and Moncef L. Nehdi[3*]

[1]School of Engineering, the University of British Columbia Okanagan
Kelowna, B.C., Canada, V1V1V7
[2, 3]Department of Civil and Environmental Engineering, the University of Western Ontario,
London, Ontario, Canada, N6A5B9

Abstract

Using superelastic shape memory alloys (SMAs) as reinforcing bars in reinforced concrete (RC) structures proved to have a great potential in seismic areas because of its recentering capability. However, using SMA bars in an entire structure is generally not economically feasible due to its high cost. Therefore, it is more practical to limit its use to the plastic hinge zones, while regular steel can be used in the other regions of the structure. Connections between SMA and steel are critical, and need to be strong enough to transfer the full force from SMA bars to steel bars. Various mechanical couplers are available in the market to splice bars in RC structures, each of which has several advantages and disadvantages. The efficiency of these couplers for connecting steel bars has been tested and reported in this paper. Since these couplers are intended for connecting steel bars only, another experimental investigation was performed to determine the suitability of these couplers for connecting SMA with steel bars. Commercially available screw-lock couplers were found to be unsuitable for connecting SMA to steel bars. An existing coupler has been modified for SMA-steel splicing to allow SMA bars to achieve their full superelastic strain. Additional tests have also been performed for connecting FRP bars to SMA bars. A new generation mechanical-adhesive type coupler was designed and developed for splicing FRP to SMA bars.

Keywords: Coupler, splicing, shape memory alloy, superelasticity, cyclic, pullout.

---

[*] Corresponding Author. Email: mnehdi@eng.uwo.ca, Fax: 519-661-3779, Phone: 519-661-2111 Ext.: 88308

Introduction

Past earthquakes demonstrated that bridges and buildings in seismic regions are susceptible to severe damage and even collapse due to excessive lateral deformations. Such infrastructure constitutes a large portion of the national wealth of any country and thus, its safety and serviceability are of great concern. Earthquake resistant structures need to be sufficiently ductile since it is not feasible to economically build structures that perform elastically under strong ground motions. Steel Reinforced Concrete (RC) structures designed according to current seismic codes are expected to behave nonlinearly to dissipate the energy input of the ground motion, while encountering permanent deformation and damage. Nevertheless, a new design philosophy aiming at maintaining the structure operational with minor repair works, even after a large earthquake, was proposed by Youssef et al. (2008).

Superelastic (SE) SMAs are unique alloys that have the ability to undergo large deformations and return to its original shape upon stress removal. This is a distinct property that makes SMA a smart material and a strong contender for use as reinforcement at critical locations in RC structures (Youssef et al. 2008). Joints are usually the weakest links in a structure during earthquake loading. In the 1994 Northridge earthquake, the main reason for failure of many structures was identified as the failure of connections of structural members (Mahid 1998). In such cases SMA material can be effectively employed in such joints to reduce the earthquake vulnerability of structures. For instance, if SMA bars are used in beam-column and column-foundation joints, they can undergo large inelastic deformation, dissipating significant amounts of energy and finally recover its deformation by its recentering capability (Ocel et al. 2004, Tamai et al. 2003).

Over the past 15 years, a substantial amount of research has been done on the material science and possible uses of SMAs in structural applications. It is being realized that SMAs possess a substantial potential to replace conventional materials, while achieving great gains in performance under seismic action. But using SMA alone as reinforcement in concrete is not currently feasible because of its high cost. It is practical to use SMA bars coupled with steel bars. SMA bars can be placed in the critical regions of the structure, particularly those subjected to excessive and repetitive deformation under severe

2

loading conditions. This should serve the purpose of reducing costs and making the RC member more ductile with high recentering capability even after reaching large deformations.

This paper provides a brief summary on the basic characteristics of SMAs and its various civil engineering applications that benefit from its superelasticity. This study focuses on the search of a suitable coupler to connect SMA with steel or FRP bars. To achieve this goal, a number of commercially available couplers have been tested. The connections between the coupler and SE SMA bar have been modified and improved in several ways, and tested under tensile load. Finally, an existing coupler has been modified for connecting SMA with steel bar, and a suitable connection has been fabricated for connecting SMA with FRP bar, which have been found quite effective up to the SE strain range of SMA bar.

Fundamentals of SMA

Shape Memory Alloys are smart and novel materials that exhibit variable stiffness and strength associated with their different polycrystalline phases. The Shape Memory Effect (SME) and Superelasticity/Pseudo-elasticity (PE) are two distinct properties that make SMA a smart material. SME is the unique phenomenon by which SMA can recover its predetermined shape by heating, even after large deformations. A SE SMA can restore its initial shape spontaneously, even from its inelastic range, upon unloading. Various compositions of SMAs such as Ni-Ti, Cu-Zn, Cu-Zn-Al, Cu-Al-Ni, Fe-Mn, Mn-Cu, Fe-Pd, and Ti-Ni-Cu have been developed and their properties have been investigated. Among these, Ni-Ti has been found to be the most appropriate SMA for structural applications because of its large recoverable strain, superelasticity and exceptionally good resistance to corrosion. In this paper, unless otherwise stated, SMAs are mainly referred to Ni-Ti SMA (commonly known as Nitinol).

At a relatively low temperature SMA exists in the martensite phase, which is soft and ductile. When heated, its stiffness and strength increase with temperature and it experiences a transformation to the austenite phase (crystalline change). In the stress (σ) free state, SMA is characterized by four distinct transformation temperatures: martensite start (M_s), martensite finish (M_f), austenite start (A_s), and

austenite finish (A_f). SMA exists in a fully martensite state when $T<M_f$ and in a fully austenite state when $T>A_f$. During the phase change from martensite to austenite and vice versa, both martensite and austenite phases coexist with temperatures between A_s and A_f, and M_s and M_f, respectively. In the martensite state when $T<A_s$, some residual strain will remain upon unloading as shown in the rightmost curve of Fig. 1. Upon heating, the material regains its original shape, known as SME. Figure 1 (the curve on the T-ε plane) shows the temperature effect on residual strain. In the austenite state (T slightly higher than A_f), six distinctive features can be recognized in the middle stress-strain curve of Fig. 1 (DesRoches et al. 2004): (a) elastic response of austenite material at low strains ($\varepsilon<1\%$) as denoted by BC; (b) stress-induced transformation from austenite to martensite with a long and constant stress plateau at intermediate strains ($\varepsilon = 1$-6%), indicated by CD; (c) elastic response in the stress-induced martensite state at large strain ($\varepsilon >8\%$) represented by DE; (d) elastic recovery of strain upon stress removal as shown by EF; (e) instinctive recovery of strain at an almost constant stress path because of the reverse transformation to austenite due to instability of martensite at $T >A_f$ as depicted by FG; and finally (f) elastic recovery in the austenite phase as indicated by GB. This exceptional property of SMA with the ability of recovering substantial inelastic deformation upon unloading yields a characteristic hysteresis loop, which is known as PE. If the temperature in the austenite phase exceeds the maximum temperature at which martensite occurs (M_d), then PE of SMA is completely lost and it behaves like an elastic-plastic material as shown in the leftmost curve of Fig. 1.

Cyclic Behavior of SMA with SE

Typical stress-strain curve of SE SMA under cyclic axial force is presented in Fig. 2. When an SMA specimen is subjected to a cycle of axial deformation within its SE strain range, it dissipates a certain amount of energy without permanent deformation. This is caused by the phase transformation from austenite to martensite during loading and the reverse transformation during unloading, ensuing a net release of energy. SMA with SE has an advantage over other common metals/alloys in the sense that

besides dissipating a considerable amount of energy under repeated load cycles, it has a negligible residual strain.

Applications of SMA

Owing to their distinct and unique properties, SMAs have been used in a wide variety of applications in different fields and industries such as aviation, medical equipment and implants. They have also been used as actuators, switches, valves and clamping devices. SMAs have also gradually gained recognition in various engineering fields. For instance, recent experimental and numerical investigations have demonstrated the possibilities of utilizing SMAs in civil engineering structures to protect buildings and bridges against earthquakes. Dolce et al. (2004) demonstrated the effectiveness of using SE SMA bracings over steel bracings for seismic retrofitting of existing RC frames. Salichs et al. (2001) and McCormick and DesRoches (2003) analytically evaluated using SE SMA bars as bracing members to reduce vibration. Indirli et al. (2001) utilized SE SMA rods for the seismic rehabilitation of a tower through the application of corrective post-tensioning forces. Inaudi and Kelly (1994), Clark et al. (1995) and others carried out analytical and experimental studies on structural response control using SE SMAs. Recent research in the application of SMAs in vibration control includes the work of Wilde et al. (2000) and others. DesRoches and Delemont (2002) and Andrawes and DesRoches (2005) performed analytical investigations on SE SMA restrainers in reducing relative hinge displacements compared to conventional restrainers. Auricchio et al. (2006) conducted numerical simulations and compared the seismic responses of three- and six-storey steel frame buildings equipped with traditional buckling-restrained steel bracings and SE SMA bracings. Their results showed that buildings with SMA bracings performed better than steel bracings in terms of inter-storey and residual drift.

Since SMA is a costly material, it was not until 2004, that it found its way as reinforcing bars in RC structures. Only two experimental research works have been reported, in which SMA bars have been used as reinforcement in RC structures subjected to cyclic loading. Saiidi and Wang (2006) used SMA rods in the plastic hinge area of RC columns and evaluated the seismic performance of these columns in

shake table tests. The results showed that SMA RC columns were able to recover nearly all of the post-yield deformation, thus requiring minimal repair. Youssef et al. (2008) and Alam et al. (2007) utilized SE SMA in the plastic hinge area of beam-column joints and conducted experimental and numerical investigations on the performance of SMA RC beam-column joints and regular steel-RC beam-column joints under reversed cyclic loading. Their results showed that SMA RC beam-column joints are advantageous over steel-RC beam-column joints because of its recentering capability even after large displacements. However, in both applications (Youssef et al. 2008 and Alam et al. 2007) SMAs were used in conjunction with regular steel and screw-lock or threaded couplers were used to connect SMA to steel bar. Machining SMA bar is difficult and costly due to its hardness. Hence, a simple, quick and economic technique needs to be developed for connecting SMA with steel bars in order to facilitate the use of SMA in critical location of RC structures.

Bar Couplers

The use of mechanical bar couplers in reinforced concrete (RC) construction has been a common, simple, swift and cost-effective method for splicing smooth and/or deformed bars under tension and/or compression. Various types of couplers (e.g. screw-lock, threaded, sleeve-filler, sleeve wedge, etc.) are commercially available for connecting bars of identical size (regular couplers) or of different standard sizes (transition couplers). Screw-lock and threaded couplers are the most commonly used for splicing steel bars. But machining large diameter bars of Ni-Ti using conventional equipments and techniques is extremely difficult due to the high hardness for SMA. Although there are various ways of welding and soldering Ni-Ti, e.g. using e-beam, laser, resistance and friction welding, and brazing with Ag-based filler metals; welding Ni-Ti to steel is much more problematic because of the brittle connection around the weld zone (Hall 2003). Weld deposits with Ni-filler metal have exhibited sufficient tensile strength allowing SE deformation of nitinol (Hall 2003). Moreover, threading large diameter bars reduces the strength of nitinol due to its sensitivity to notches. Although Cu-based SMAs like Cu-Zn-Al and Cu-Al-Ni are less costly, they display poor ductility. Fe-Mn-Si-based low-cost alloys have been found to exhibit

good mechanical properties with a wide transformation hysteresis, good machinability and weldability as well as good workability compared to nitinol. Fe-based SMAs may also have good bond strength compared to that of Ni-Ti, if used as reinforcing bars in RC structures. Problems related to these alloys include poor shape recovery and lower shape recovery stress than that of Ni-Ti-based SMAs. Therefore, screw-lock couplers appear to be the most suitable for connecting SMA with steel bar since they do not require the ends of bars either to be threaded or specially treated. Likewise, no special installation equipment is required; quick and easy installation save time and money, which is ideal for new construction, rehabilitation, retrofitting, strengthening and upgrading of RC structures alike.

The screw-lock couplers used in this study are mechanical splices and connectors compatible with reinforcing bars (Barsplice Products 2006, Dayton/Richmond Concrete 2006) that comply with ASTM A 615 (2007), ASTM A 706 (2007), and ASTM A 996 (2007). They consist of smooth steel sleeves with converging sides. Two different types of screw-lock couplers have been used for connecting bars: a) regular single barrel coupler (SBC), and b) double barrel transition coupler (DBTC) (Barsplice Products 2006, Dayton/Richmond Concrete 2006). In SBC, the reinforcing bars are inserted into the coupler ends until it reaches the pin at the middle (center stop). Both the bars meet head to head, separated by the pin at the middle, as shown in Fig. 3. In the case of DBTC, the bars are inserted into two different slots of the coupler ends, and instead of meeting head to head; they meet in parallel, as shown in Fig. 4.

Pullout Tests of Couplers with Steel Bars

First, simple pullout tests have been performed to determine the tensile resistance/capacity of the couplers. Based on these tests, a suitable coupler is chosen. The cyclic tensile behavior is studied for the selected coupler.

Splicing Mechanism and Test Setup

Both types of couplers tested in this study have a series of cone-pointed hexagonal-head lock shear screw bolts arranged along the longitudinal axis of the bar (as shown in Figs. 3 and 4). These bolts are threaded into the side of seamless tubing. The SBC has two serrated steel strips along its full length and the DBTC has converging sleeve sides, as shown in Figs. 3 and 4, respectively. During mechanical splice assembly, the heads of the shear bolts are tightened by a power or a hand-held ratchet wrench. The tightening embeds the shear bolts into the bar surface and wedges the bar into the serrated steel strips for converging sleeve sides. Screw heads shear off (Fig. 5) when tightened to the prescribed installation torque as specified in the manufacturer's manual (Barsplice Products 2006). Forces from the shear bolts cause bar deformations to interlock the bar within the coupler wedge. Thus, the resistance from the shear bolts and the wedge action results in a full positive connection for transferring tension and/or compression forces from bar to bar.

Instead of testing the entire arrangement, i.e. inserting two bars from the opposite end of the coupler (Fig. 2), the test was done by inserting one bar at a time. After inserting a bar in one end of the coupler, the heads were sheared off by applying the prescribed torque. The coupler arrangement was then tested in a universal testing machine under tension only. The spliced bar was inserted through a thick circular steel plate, which acted as a reaction plate for the coupler that allows pulling the bar in tension as shown in Fig. 6. An LVDT attached to the bar was placed on the circular plate to measure the bar slip from the coupler (Fig. 6). Since the LVDT was attached to the bar, the slippage value was corrected by deducting the bar elongation from the measured slippage. This preliminary simple test was conducted to determine the best possible option to connect the SMA bar to a steel rebar so as to optimize the use of the SMA bar by locating it in the hinge area. Since joints in RC structures are made more rigid than the jointed members, during loading, the couplers located within the joint will be pulled against concrete, and thus, subjected to compressive stresses. Conversely, in the case where the couplers are placed within an RC member (not in a joint), they may be subjected to tension along with the rebar. Similar restrained tension tests of DBTC

couplers were conducted by Coogler et al. (2008). Their results show that splices perform better in restrained tension tests compared to that of direct tension tests.

Test Results

First, tensile strength tests have been performed for the bars that will be spliced. The results are shown in Table 1. The coupler specimens described in the previous section were tested under tension. The results are shown in Table 2 where the specimens are designated as D-2-T1-1, R-1-T2-3, etc. The first alphabet represents whether the bar is a deformed bar (D) or a round (smooth with no deformation) bar (R), the second part represents the diameter of the bar where 1, 2 and 3 stand for 12.75, 16 and 19.5 mm diameter bars, respectively. The third part represents the type of coupler, where T1 and T2 represent SBC and DBTC, respectively, and the last digit represents the specimen number for similar arrangements. Examples of load resistance and bar slip relationship for different specimens are shown in Fig. 7.

Discussion

The test results presented in Table 2 show that SBCs can produce full ultimate strength of both deformed bars and round bars. The bar slip at yielding was found to be relatively small for all SBC coupled specimens compared to those of all DBTC coupled specimens, which proves SBC to be adequate for coupling the bars. All SBC coupled specimens failed by rupture of bars (Figs. 7 and 8a) and provided sufficient ductility. The results indicate that SBC can provide continuity along the bar. Conversely, all 15M bar specimens connected with DBTCs failed to produce the ultimate strength of the bars. After reaching the yield point, there was no increase in the load, which rather dropped suddenly and the connection failed by the bolt screws inducing shearing along the bar. Typical tearing of the failed bar along its length is shown in Fig. 8b. In the case of splicing round bars with DBTC, although all bars could reach its yield strength, two failed by rupture, and one bar failed at the coupler by pulling off the bar splice. Thus, DBTCs exhibit a lack of ductility, which may result in little warning and possible sudden failure. SBC was found herein to be a better candidate than DBTC for splicing bars.

The stress-slip relationship is linear up to f_y, except for cases where failure occurrs prior to reaching f_y (Fig. 7). After yielding, the slip increased significantly and often exceeded 20 mm. Different requirements are being used for evaluating the performance of mechanical splices. In most cases, if the tensile capacity of a mechanical splice exceeds 1.25f_y, it satisfies the splicing requirement (ACI 318-08, AASHTO LRFD 2004). However, this might not be possible if the ultimate strength of a bar is less than 1.25f_y, which is the case for 15M rebar as shown in Table 2. Therefore, those couplers that can achieve the ultimate strength of a rebar should also qualify for mechanical splicing of such rebar. Each result in Table 2 shows that the slip at a stress of ½ f_y was less than 0.25 mm as required by AASHTO LRFD (2004) to qualify for mechanical splicing.

Pullout Tests of Couplers Connecting SMA to Steel Bars

This section presents the cyclic tensile behavior of SMA bars connected by SBCs. Figure 9 shows a typical tensile strength test result of SMA bar. The stress-strain curve is composed of linear branches which are connected by smooth curves. The linear branches are assumed to intersect at points (as shown in Fig. 9) to determine its characteristic strength and strains. The first yield point is identified as 401 MPa (f_y) at 0.75% strain (ε_y). The SE strain (ε_{SE}) is identified as 6.4% at a stress of 503 MPa (f_{SE}). Its initial Young's modulus (E_y) is calculated as 62.5 GPa. The grips' teeth of the test machine firmly held the SMA bar as the stress increased during the pullout test. This biting effect created notches on the SMA bar surfaces, which caused failure of the bar at the grip.

Splicing Mechanism, Test Setup and Results

The splicing mechanism with SBC described in the previous section has been modified for connecting SMA bars. Several attempts have been made to develop a proper connection that can withstand cyclic tensile loads up to the SMA's SE strain range, which will be the required criteria for a coupler to qualify as a mechanical splicer in seismic regions. In each case SBC was connected with 20.6 mm diameter SMA bar at one end and 22M steel bar at the other end.

Case 1

SBC without any modification was first used for connecting SMA bars. The tightened shear bolts were embed into the SMA bar surface (Fig. 5) and applied normal forces on the bar holding it onto the serrated steel strips (Fig. 3). The cyclic tensile strength test result for Case 1 is shown in Fig. 10 (a). In this case, the SMA bar failed after four load cycles at a strain of 1.48%. During specimen preparation, as the heads of the shear bolts were tightened they embedded into the SMA bar surface producing notches. As a result, the strength of SMA decreased due to its sensitivity to notches, leading to premature bar failure.

Case 2

When Case 1 was found unsuitable for connecting SMA bar, several attempts were made to avoid creating perforations into SMA bar. In case 2, a similar mechanism has been used for SBC, except the use of an additional metal strip, which has been placed underneath the screw bolts over the SMA bar as shown in Fig. 11 (a). The thickness of the strip was chosen such that the sharp ends of the screw bolts will penetrate the steel strip but will not touch the surface of the SMA bar. Thus, the pullout strength of the coupler will mainly depend on the friction of the SMA bar produced by the axial forces from the screw bolts. However, Case 2 was also ineffective as it failed to produce a single cycle in the pullout test. The SMA bar did not reach its yield strength as it slid out of the coupler at a stress of 386 MPa.

Case 3

In this case, two extra rows of holes were drilled through the coupler in parallel to the existing row at an angle of 45º away from the centre of the coupler, as shown in Fig. 11 (b, c, d). Thus, nine screw locks were used to connect the SMA bar to the coupler. All the sharp ends of the screws have been flattened to a diameter of 2 mm. Case 3 was somewhat effective as it produced eight cycles in the pullout test before failure of the connection (Fig. 10 (b)). In this case the SMA bar slide out from one end of the coupler, and

the steel bar on the other end experienced some slippage. The SMA bar experienced a maximum strain of 3.22% and a residual strain of 0.36%.

Case 4

This case is similar to Case 3. The difference is that the two extra rows of holes drilled through the coupler in parallel to the existing row are at an angle of 60º (instead of 45º) away from the centre of the coupler. Moreover, two extra holes were drilled for the steel bar at the same angle. The other difference is that the sharp ends of the screws have been flattened further, i.e. 3.5 mm in diameter. Case 4 was found most effective for connecting SMA bar with steel bar using SBC. This arrangement could produce strains up to the full SE range of SMA. Figure 10 (c) shows the cyclic tensile strength of SMA bar in this connection. The bar experienced a maximum of 6.38% strain and a residual strain of 0.73%. The connection was subjected to eleven load cycles before failure occurred. The SMA bar failed at the connection end of the coupler (Fig. 11d) possibly due to high stress concentration (Fig. 11e) and micro-crack formation at the point of contact of coupler screws, which ultimately caused formation of notches and failure. A simple pullout test was also performed to determine the slippage of SMA bar inside the coupler, and the result is illustrated in Fig. 12. In total, four pullout tests have been performed (case 4) and the results are presented in Table 3. The average slip at f_y is 2.35 mm with a standard deviation of 0.30 mm, whereas the slip at a stress of f_{SE} is 10 mm with a standard deviation of 1 mm.

Pullout Test of Couplers Connecting SMA to FRP Bars

Fiber reinforced polymer (FRP) bars have been introduced in the construction industry to eliminate problems associated with steel corrosion. However, FRP is a brittle material. As a result, concrete structures reinforced with FRP bar do not generally provide adequate ductility before failure. But if FRP bar can be used in conjunction with a ductile material such as stainless steel or SMA, it may not only eliminate corrosion problems but could also provide adequate ductility and warning before failure.

Therefore, an attempt has been made in the present study to connect FRP and SMA bars. This should facilitate the development of corrosion free and ductile hybrid reinforcement.

There is no mechanical coupler readily available that can connect brittle FRP bar to other ductile materials such as steel bars. It is not possible to splice FRP to steel bar using a mechanical coupler consisting of regular SBC since the sharp ends of screws will rupture the top fibres of the GFRP bar. SBC with flattened screws will not work either, as the FRP bar will not be able to sustain normal forces in the perpendicular direction of the orientation of fibres, and the fibres will get easily damaged. Therefore, a viable option was to use an adhesive type coupler for the FRP bar. Two types of FRP bars were considered: one with sand coating and the other without sand coating. Also, two different types of epoxy adhesives were used for connecting FRP to steel. The first is a multipurpose structural bonding and grouting epoxy adhesive (epoxy 1, Epogrip), and the second is a concrete bonding adhesive (epoxy 2, Concresive).

Since FRP bar cannot be held directly by the grip of the universal testing machine, both sides of FRP bars were required to be connected with a coupler, and each end of the coupler/pipe was connected to steel or SMA bar (Figs. 13 and 14). Figure 13 shows three types of couplers used for the splicing of FRP bars. The first is a SBC coupler, the second is a steel pipe of 250 mm long connected to SBC by welding, and the third is a 340 mm long stainless steel pipe welded to a SBC.

For SBCs, two cases were considered. In the first case, FRP bar was connected to SBC with epoxy adhesive only, whereas in the second case, FRP bar was connected both with epoxy adhesive and screws. In both cases, two types of epoxy adhesive were tested. For case 1, two types of FRP bars were considered: one with sand coating and the other without sand coating. In the second case, flattened screws were used, which were tightened after curing the epoxy adhesive in order to apply normal forces on the FRP surface so as to increase its frictional resistance against slip. The tightening of the screws was controlled to avoid rupture of the fibres.

Figure 15 shows pullout test results in terms of stress versus slippage of uncoated FRP bar from the SBC coupler. The results depict that epoxy 2 could resist higher tensile load compared to epoxy 1. In

both cases the slippage was negligible at the initial stage of loading. There was a sudden drop in load resistance after reaching the peak load. Increased slippage was observed in the second branch of the curve after its peak resistance. However, more than 80% of the drop in the tensile load could be gradually recovered with the increase of slippage of the FRP bar as shown in Fig. 15. When using the epoxy 1, the tensile load resistance of the FRP bar (second branch of the curve) could reach its peak at the expense of higher slippage compared to the epoxy 2 (Fig. 15a and 15b).

Figure 16 shows pullout test results of a sand coated FRP bar. The results demonstrate that the epoxy 1 could resist higher tensile load compared to that of the epoxy 2. However, slippage was higher for epoxy 1 than that for epoxy 2. There was a sudden drop in load resistance which was not recoverable as the bar pulled out of the coupler as shown in Fig. 17. It was observed that at the initial loading stage, the sand coating provided good bonding with the surrounding epoxy. As the load increased, the interface between the sand grains and the bar debonded causing inter-laminar shear failure (Maruyama et al. 1989). This type of anchorage failure could be avoided by providing additional development length.

Figure 18 shows the pullout test results of sand coated FRP bars anchored to SBC with epoxy and flattened screws. The stress versus slippage results depict that the epoxy 1 could resist higher tensile load compared to that of the epoxy 2. In both cases the slippage was negligible up to the peak tensile load. After reaching its peak, the load gradually dropped with an increase in the slippage of the FRP bar. Thus, Case 2 shows a better performance compared to Case 1, i.e. the use of flattened screws increased the pullout resistance and improved the failure pattern, with no sudden failure.

It was observed from the test results that in the case of splicing of sand coated FRP bar, epoxy 1 provided better pullout resistance compared to that of epoxy 2. However, the required tensile load resistance could not be achieved during the pullout test of the spliced FRP bar due to inadequate development length of the FRP bar inside SBC. This can be improved using a larger development length. Hence, this was tested with two pipes of different length, each welded to SBC. Figure 19 (a) and (b) show stress versus slippage for a sand coated FRP bar spliced to 250 mm and 340 mm long pipes, respectively, using epoxy 1. The results clearly show that larger development length improved the pullout resistance of

the spliced FRP bar. 340 mm long steel pipe could increase the load resistance by about 38% compared to that of a 250 mm long steel pipe. Sudden anchorage failure was observed in the case of the 250 mm long pipe, whereas a gradual failure was observed using the 340 mm long pipe. Figure 19 (b) also shows that the spliced connection could develop full superelastic strain of the SMA bar (Fig. 10c).

Economic Considerations

Although there is a substantial potential for utilizing SMA as reinforcement in RC structures, the cost of this material is a primary restraining factor to a larger implementation of SMA in structural applications. The price of SMA (Ni-Ti) has been significant reduced in the last ten years, from more than $1000 USD to below $100 USD per kg at present. Like FRPs, it is expected that the more widely it will be used, the more its price will decrease. Incorporating SMA in a frame building will not only increase the material cost, but also the costs associated with couplers and labour charges for splicing SMA to steel. An eight storey office building with plan dimensions of 18-m by 18-m having 4 bays in both directions was designed with a moderate level of ductility. The total project cost (including materials, labour, electrical and mechanical) was estimated. It was found that using SMA will increase the total cost by 5%, whereas an additional 2.6% cost increase will be associated with the use of mechanical couplers and the related labour charges for splicing SMA to steel rebar. However, if SMA can be employed in hybrid system along with steel bar, the cost may become competitive for important RC structures susceptible to earthquake risk. The feasibility of using SMA materials and devices in full-scale construction projects has been studied by Bruno and Valente (2002). They considered various costs in their study including direct (structural, nonstructural) and indirect (injuries and deaths) in the construction phase and also when induced by earthquake events. The cost of SMA-based devices turned out to be of the same order as that of conventional steel devices. SMA is also highly resistant to corrosion. Plastic hinge regions suffer most cracks in RC structures. If SMA is placed at the plastic hinge zones, it will not experience significant corrosion. Under strong ground motion, SMA may experience inelastic deformation, but unlike steel, it will regain its original length after the earthquake because of its strong recentering capability; thus,

keeping the structure serviceable, requiring minimum amount of repairing. SMAs have been found much preferable in the sense that they do not require additional costs such as for maintenance or replacement. The efficiency of SMA devices is unique in reducing economic losses and minimizing human risk associated with natural disaster events. The present research on coupling SMA to steel and FRP bar paves the way for future research on using SMA in hybrid reinforced systems that are less costly, but ductile and resistant to corrosion.

Conclusions

Because of its higher cost compared to that of other construction materials, SMAs are not currently expected to be used alone as longitudinal bars in RC structures; rather it would be used along with steel bars in a hybrid system. This paper provides a novel approach to connect SMA with steel and FRP bar. The objective of this study is to develop suitable couplers for such connections where SMA bars can be effective beyond its SE strain range under cyclic loading. Screw-lock couplers have been found appropriate for connecting SMA to steel bar since it requires no special installation equipment or modification/special treatment for the bar. It is also quick and easy to install, saving time and money, which is ideal for new construction, rehabilitation, retrofitting, strengthening and upgrading of RC structures. Two types of screw-lock couplers have been tested under simple pullout test. SBC has shown better performance compared to that of DBTC in terms of load resistance and ductility. SBC also provided a direct, in-line load transfer mechanism. DBTC may also prove to be impractical, since it can cause congestion of the reinforcement cage.

Regular SBCs were used in this exploratory study on SMA and steel bar connections. It was found that regular SBCs are not sufficient to hold SMA bar up to its full SE strain range. Several alternatives were examined so as to modify SBC to achieve better performance. Several combined modifications to the SBC allowed achieving SMA's full superelastic strain. Two parallel extra rows of shear bolts/screws at an angle of 60º from the centre row (i.e. 9 screws) were needed to hold a single SMA bar in which all screw ends were flattened to a radius of 3.5 mm. Two extra screw bolts were also

used to connect the steel bar. The modified version of SBC showed good performance under cyclic tensile loading up to its superelastic strain range.

SBC was also used to splice SMA to FRP bar. The test results showed that mechanical anchorages are not suitable for connecting FRP bar and that adhesive type couplers should be used. The proposed coupler that splices SMA to FRP consists of a steel tube welded to SBC. The steel tube connects the FRP bar with an epoxy adhesive, and SBC connects the SMA or steel bar. Three different tube lengths were considered for connecting the FRP bar using epoxy. It was observed that larger development length and a length of $18d_b$ (d_b = diameter of FRP bar) can produce sufficient tensile force to stress the SMA bar up to its superelastic strain range.

The test results demonstrate that SMA possesses a great potential to be used as reinforcement at critical regions of RC structures along with conventional steel, where SMA is expected to yield under strains caused by seismic loads, which will not only dissipate significant amount of energy, but also potentially recover deformations at the end of earthquake. Thus, smart RC beam-column joints for buildings, and column-foundations for bridges can be built with superelastic SMA bar, allowing structural engineers to design connections for low/moderate shear distortions and rotations that exhibit little damage, and mitigate post earthquake joint repairs. The SMA/FRP connections open the door for introducing ductility in FRP reinforced concrete structures. Stainless-steel and SMA can be used in the hinge locations of FRP RC structures, thus providing ductility. Hence, hybrid FRP-SMA-steel reinforced concrete structures that are both cession free, resistant to seismic loading, and having post-earthquake residual deformations can be developed.

Acknowledgement

References:

A615/A615M-06a (2007). "Standard specification for deformed and plain carbon-steel bars for concrete reinforcement." West Conshohocken (PA), ASTM Intl 2007.

A706/A706M-06a (2007). "Standard specification for low-alloy steel deformed and plain bars for concrete reinforcement." West Conshohocken (PA), ASTM Intl 2007.

A996/A996M-06a (2007). "Standard specification for rail-steel and axle-steel deformed bars for concrete reinforcement." West Conshohocken (PA), ASTM Intl 2007.

AASHTO LFRD, 2004, "Bridge Design Specifications," third edition, American Association of State Highway and Transportation Officials, Washington, DC, 1522 p.

ACI Committee 318, 2005, "Building Code Requirements for Structural Concrete (ACI 318-05) and Commentary (318R-05), American Concrete Institute, Farmington Hills, MI, 430 p.

Alam, M. S., Youssef, M. A., and Nehdi, M. (2007). "Seismic behaviour of concrete beam-column joints reinforced with shape memory alloys." Ninth Canadian Conf. on Earthquake Engg., Ottawa, Canada, 2007. 10p.

Andrawes, B., and Desroches R. (2005). "Unseating prevention for multiple frame bridges using superelastic devices." Smart Materials and Structures 2005; , 14(3), :S60-S67.

Auricchio, F., Fugazza, D., and DesRoches, R. (2006). "Earthquake performance of steel frames with Nitinol braces." J. of Earthquake Eng.,g 2006; 10(SPEC),: 45-66.

Barsplice Products Inc. (2006). "Zap screwlok ® Mechanical splices and connectors for reinforcing bars – review." April 2006, available at: http://www.barsplice.com/BPI_Scans/Zap_Data-Sheet_RevA.pdf.

Bruno, S., and Valente, C. (2002). "Comparative response analysis of conventional and innovative seismic protection strategies." Earthquake Eng.g and Struct. Dyn., 2002; 31(5), :1067-1092.

Clark, P. W., Aiken, I. D., Kelly, J. M., Higashino, M., and Krumme, R. (1995). "Experimental and analytical studies of shape-memory alloy dampers for structural control." The Proc of SPIE, 1995; 2445, :241-251.

Coogler, K.L., Harries, K.A., and Gallick, Marcella. (2008). "Experimental study of offset mechanical lap splice behavior," ACI Structural Journal, 105(4), 478-487.

Dayton/Richmond Concrete Accessories (2006). "Bar-lock coupler system." April 2006, available at: http://www.daytonconcreteacc.com.

DesRoches, R.,, and Delemont, M. (2002). "Seismic retrofit of simply supported bridges using shape memory alloys." Engineering Structures, 2002; 24(3), :325-332.

DesRoches, R., McCormick, J., Delemont, M. (2004). "Cyclic properties of superelastic shape memory alloy wires and bars.", ASCE J. of Struct. Engg. 2004;, 130(1), :38-46.

Dolce, M., Cardone, D., Marnetto, R., Mucciarelli, M., Nigro, D., Ponzo, F. C., and Santarsiero, G. (2004). "Experimental static and dynamic response of a real RC frame upgraded with SMA re-centering and dissipating braces." The Proc of the 13th World Conf on Earthquake Engg, 2004; Paper no. 2878.

Hall, P. C. (2003). "Laser welding Nitinol to stainless steel." Proc.eedings of Intl. Conf. on Shape Memory and Superelastic Technologies, California, 2003; 219-228.

Inaudi, J. A., and Kelly, J. M. (1994). "Experiments on tuned mass dampers using viscoelastic, frictional and shape memory alloy materials." The Proc 1st World Conf on Structural Control, 1994, ; 2(TP3),: 127-136.

Indirli, M., Castellano, M. G., Clemente, P., and Martelli, A. (2001). "Demo-application of shape memory alloy devices: the rehabilitation of the S. Giorgio Church Bell-Tower." Proc of SPIE, 2001,; 4330, :262-272.

Mahin, S. A., (1998). " Lessons from damage to steel buildings during the Northridge earthquake." Eng.ineering Struct.,ures 1998; 20(4-6),: 261-270.

Maruyama, T., Itoh, S., and Nishiyama, H. (1989). "Study on bond characteristics of deformed fibre reinforced plastic rods." Proceedings . of the Japan Concrete Institute 1989;, 11(1), :777-782.

McCormick, J., and DesRoches, R. (2003). "Seismic response using smart bracing elements." Proc of the Extreme Loading Conference, Toronto, 2003.

Ocel, J., DesRoches, R., Leon, R.T., Hess, W. G., Krumme, R., Hayes, J. R., and Sweeney, S. (2004). "Steel beam-column connections using shape memory alloys." ASCE J. of Struct. Eng.,g, 2004; 130(5), :732-740.

Saiidi, M. S. and Wang, H. (2006). "Exploratory study of seismic response of concrete columns with shape memory alloy reinforcement," ACI Structural Journal, 103(3), 436-443.

Salichs, J., Hou, Z., and Noori, M. (2001). "Vibration suppression of structures using passive shape memory alloy energy dissipation devices.", Journal. of Intel. Mat. Systems. and Struct., 2001; 12(10),: 671-680.

Tamai, H., Miura, K., Kitagawa, Y., and Fukuta, T. (2003). "Application of SMA rod to exposed-type column base in smart structural system." The Proc of SPIE, 2003,; 5057,: 169-177.

Wilde, K., Gardoni, P., and Fujino Y. (2000). "Base isolation system with shape memory alloy device for elevated highway bridges." Engineering Structures,Courses 2000; 22,: 222-229.

Youssef, M. A., Alam, M. S., and Nehdi, M. (2008). "Experimental investigation on the seismic behaviour of beam-column joints reinforced with superelastic shape memory alloys." Journal. of Earthquake Engineering 2008; ., 12(7),: 1205-1222.
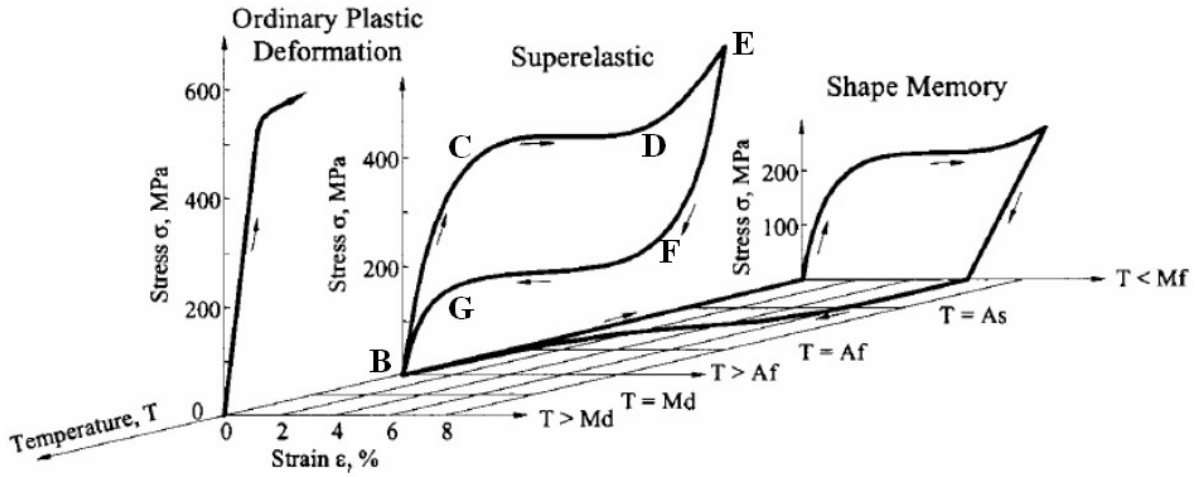
LIST OF FIGURES

Figure 1. 3D stress-strain-temperature diagram of SMA showing SME in martensite phase, SE in austenite/martensite phase transformation, and elastic-plastic behavior of austenite at higher temperature (DesRoches et al. 2004, with permission).
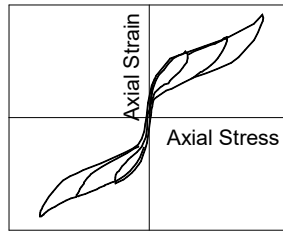
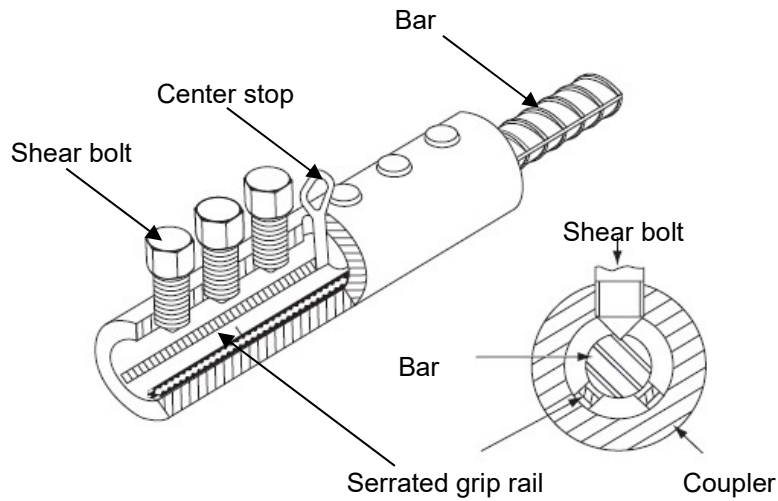Fig. 2. Typical stress-strain diagram of SE SMA under cyclic axial load.

Fig. 3. Regular single barrel screw-lock coupler (Barsplice Products 2006, Dayton/Richmond Concrete 2006 with permissions)
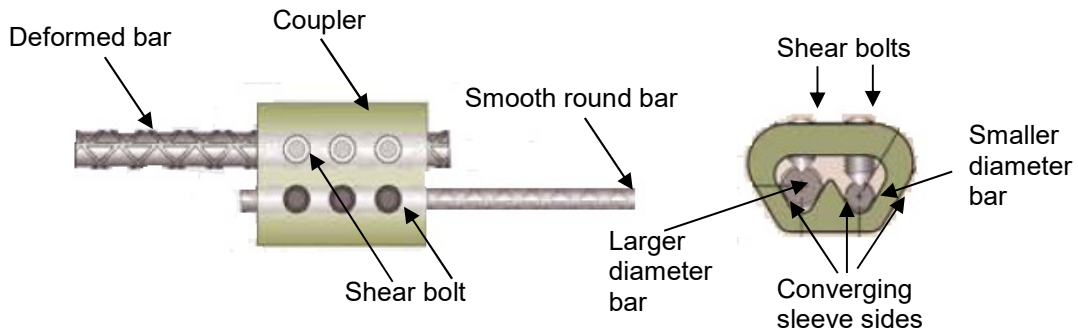
Fig. 4. Double barrel zap transition screw-lock coupler (Barsplice Products 2006, Dayton/Richmond Concrete 2006 with permissions).
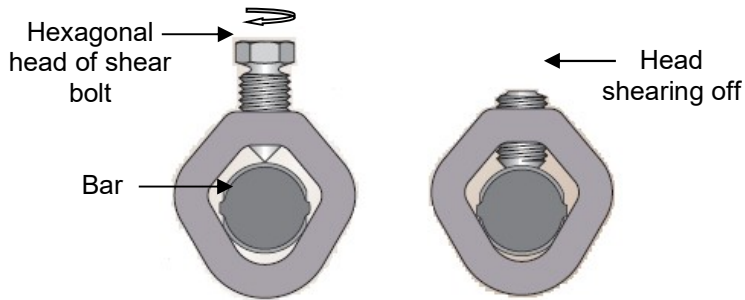
Fig. 5. Screw heads shearing off by applying the tightening torque (Barsplice Products 2006, Dayton/Richmond Concrete 2006 with permissions).
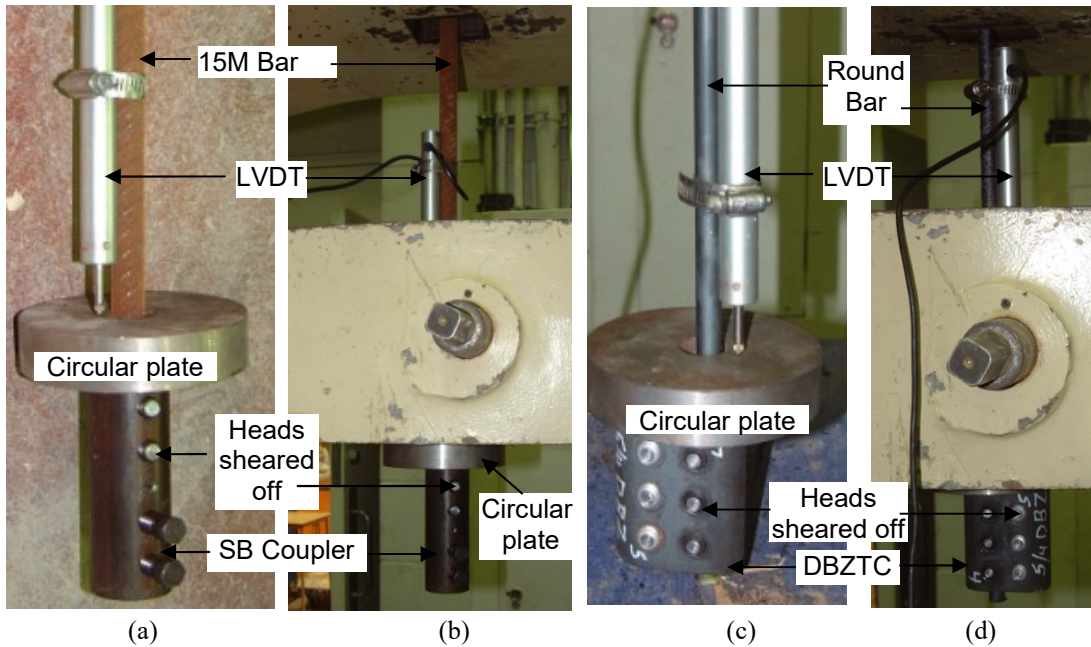
Fig. 6. a) Test set up for pullout test of bar coupled with SBC, b) bar coupled SBC in UTM, c) test set up for pullout test of bar coupled with DBTC , d) bar coupled DBTC in UTM.

Fig. 7. Load resistance and bar slip relationship of specimens a) R-1-T1-1, b) R-1-T2-2, c) D-2-T1-1, d) D-2-T1-3, e) D-2-T2-1, f) D-2-T2-2, g) D-3-T1-1 and D-3-T1-2.

Fig. 8. Failure pattern of bar in a) SBC, and b) DBTC.

Fig. 9. Tensile strength test result of SMA bar.

Fig. 10. Cyclic tensile strength of SMA bar in SBC for (a) Case 1, (b) Case 3, and (c) Case 4.

Fig. 11. (a) Coupler arrangement of SMA bar in SBC (Case2), (b) SBC for splicing SMA and steel bar (Case 3), (c) screws with sharp and flat ends used for splicing steel and SMA bar respectively (Case 3 and 4), (d) arrangement of screws in SBC at an angle of 45º (Case 3) or 60º (Case 4) from the centre row, also showing the failure of SMA bar at the connection (Case 4), and (e) SMA bar after failure from the coupler (Case 4).

Fig.12. Stress versus slippage of SMA bar inside coupler (Case 4).

Fig. 13. Epoxy adhesive connecting FRP bar to (a) SBC (b) 250 mm long steel pipe and (c) 340 mm long stainless steel pipe (screw lock-adhesive type coupler) with their ends connected to steel bar.

Fig. 14. Test setup for pullout test of FRP bar in (a) SBC coupler, (b) 250 mm long steel pipe, (c) 340 mm long stainless steel pipe (screwlock-adhesive type coupler).

Fig. 15. Uncoated FRP bar connected to SBC using (a) epoxy 1 (Epogrip), and (b) epoxy 2 (Concresive).

Fig. 16. Sand coated FRP bar connected to SBC using (a) epoxy 1 (Epogrip), and (b) epoxy 2 (Concresive).

Fig. 17. Sand coated FRP bar connected to SBC with flattened screws and epoxy adhesives (a) failure pattern of FRP bar, and (b) inner face of epoxy adhesive inside coupler after pullout of FRP bar.

Fig. 18. Sand coated FRP bar connected to SBC with flattened screws and epoxy adhesives of (a) epoxy 1 (Epogrip), and (b) epoxy 2 (Concresive).

Fig. 19. Sand coated FRP bar connected with epoxy 1 (Epogrip) to (a) steel pipe (250 mm long), and (b) stainless steel pipe (340 mm long).

LIST OF TABLES

Table 1: Tensile strength test results of steel bars

Table 2: Pullout test results of couplers splicing steel bar

Fig. 1. 3D stress-strain-temperature diagram of SMA showing SME in martensite phase, SE in austenite/martensite phase transformation, and elastic-plastic behavior of austenite at higher temperature (DesRoches et al. 2004 with permission).

Fig. 2. Typical stress-strain diagram of SE SMA under cyclic axial load.

Fig. 3. Regular single barrel screw-lock coupler (Barsplice Products 2006, Dayton/Richmond Concrete 2006 with permissions)

Fig. 4. Double barrel zap transition screw-lock coupler (Barsplice Products 2006, Dayton/Richmond Concrete 2006 with permissions).

Fig. 5. Screw heads shearing off by applying the tightening torque (Barsplice Products 2006, Dayton/Richmond Concrete 2006 with permissions).

(a)   (b)   (c)   (d)

Fig. 6. a) Test set up for pullout test of bar coupled with SBC, b) bar coupled SBC in UTM, c) test set up for pullout test of bar coupled with DBTC , d) bar coupled DBTC in UTM.

Fig. 7. Load resistance and bar slip relationship of specimens a) R-1-T1-1, b) R-1-T2-2, c) D-2-T1-1, d) D-2-T1-3, e) D-2-T2-1, f) D-2-T2-2, g) D-3-T1-1 and h) D-3-T1-2.

(a)

(b)

Fig. 8. Failure pattern of bar in a) SBC, and b) DBTC.
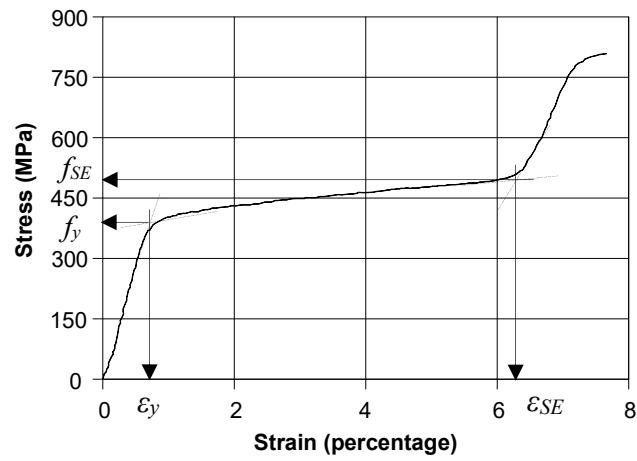
Fig. 9. Tensile strength test result of SMA bar.
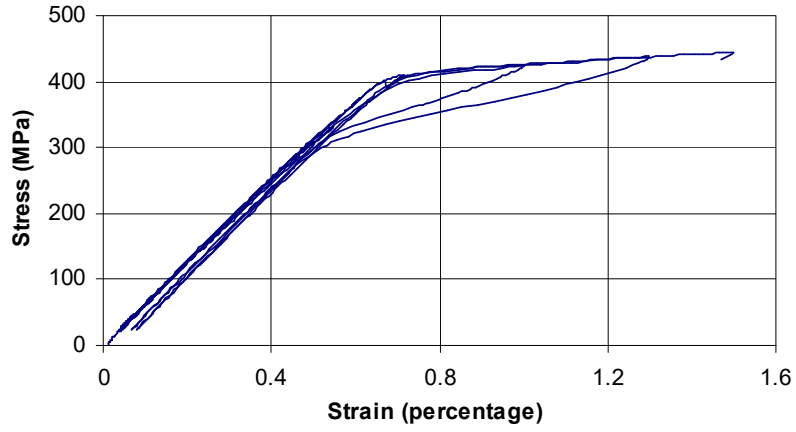
(a)
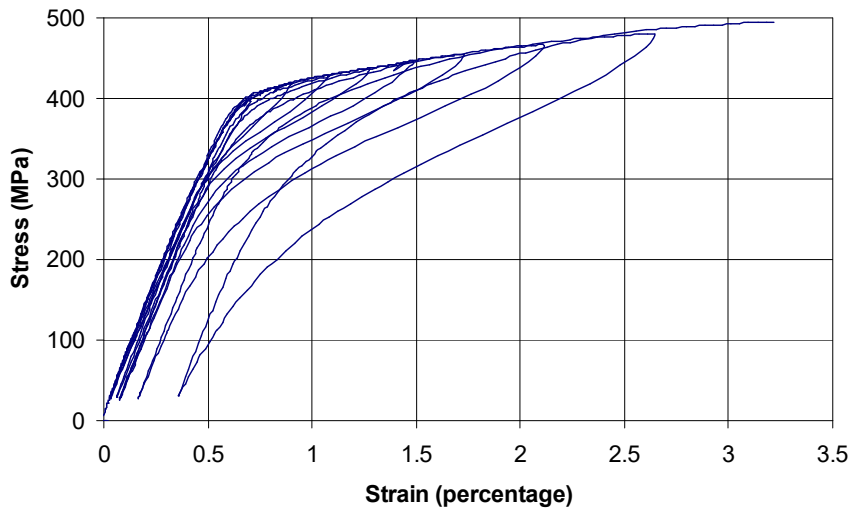
(b)
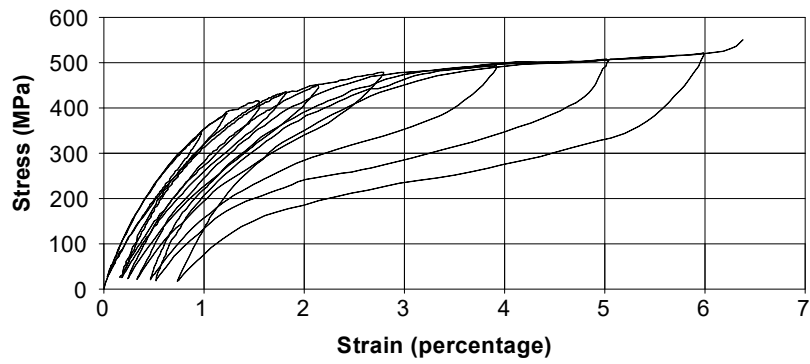
(c)

Fig. 10. Cyclic tensile strength of SMA bar in SBC for (a) Case 1, (b) Case 3, and (c) Case 4.
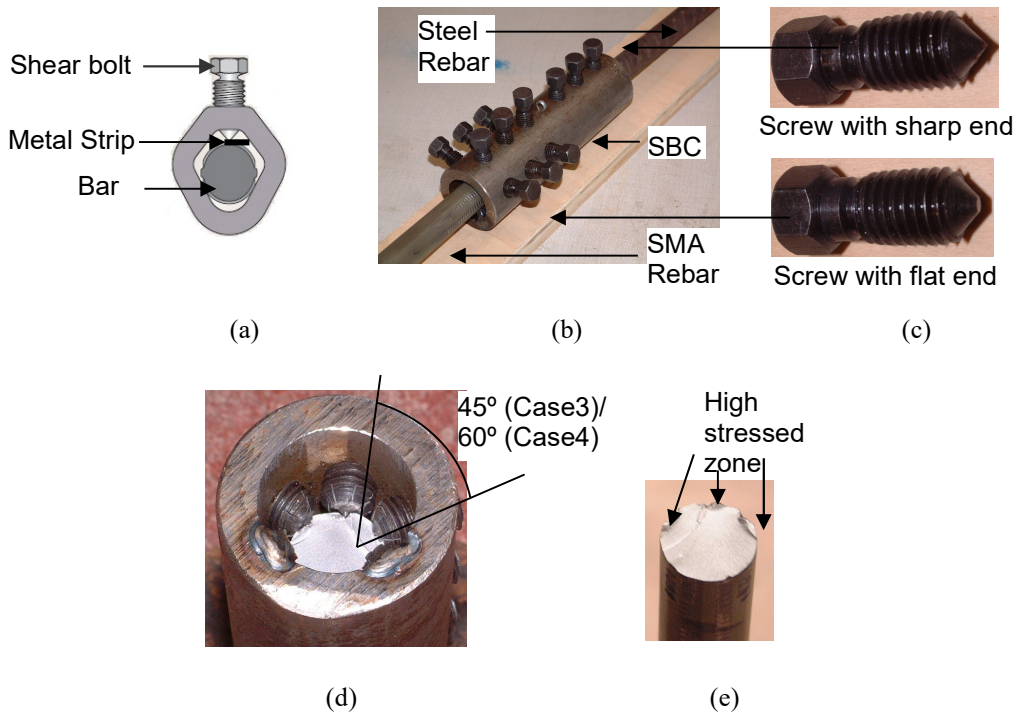
Fig. 11. (a) Coupler arrangement of SMA bar in SBC (Case2), (b) SBC for splicing SMA and steel bar (Case 3), (c) screws with sharp and flat ends used for splicing steel and SMA bar respectively (Case 3 and 4), (d) arrangement of screws in SBC at an angle of 45º (Case 3) or 60º (Case 4) from the centre row, also showing the failure of SMA bar at the connection (Case 4), and (e) SMA bar after failure from the coupler (Case 4).
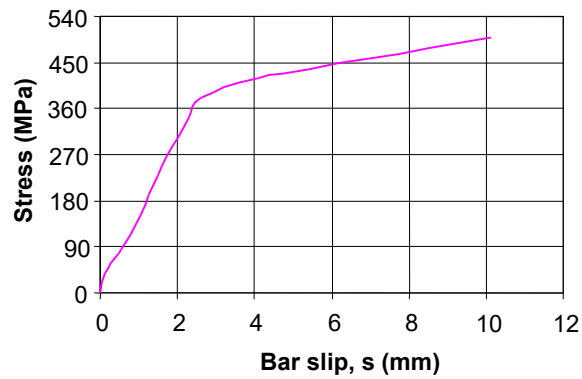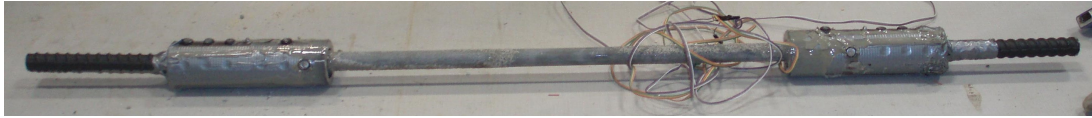

Fig.12. Stress versus slippage of SMA bar inside coupler (Case 4).

(a)

(b)

(c)

Fig. 13. Epoxy adhesive connecting FRP bar to (a) SBC (b) 250 mm long steel pipe and (c) 340 mm long stainless steel pipe (screwlock-adhesive type coupler) with their ends connected to steel bar.

(a)   (b)   (c)

Fig. 14. Test setup for pullout test of FRP bar in (a) SBC coupler, (b) 250 mm long steel pipe, (c) 340 mm long stainless steel pipe (screwlock-adhesive type coupler).
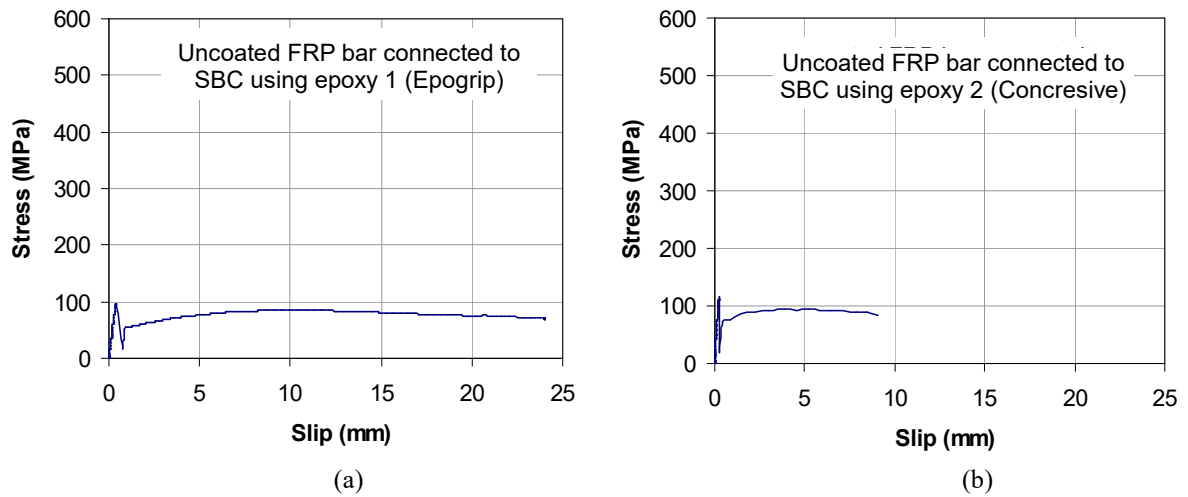
Fig. 15. Uncoated FRP bar connected to SBC using (a) epoxy 1 (Epogrip), and (b) epoxy 2 (Concresive).
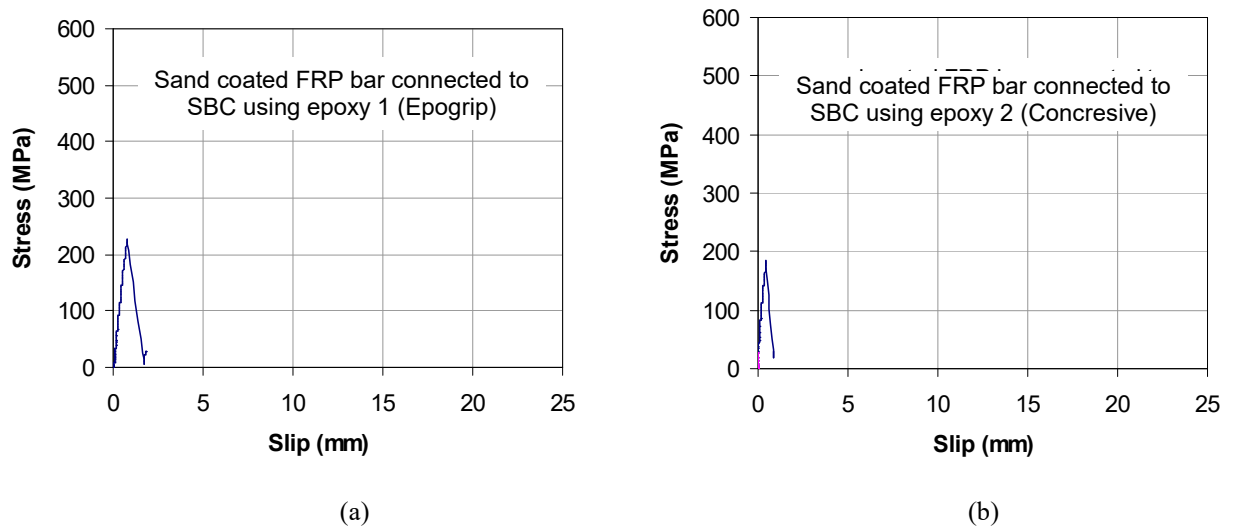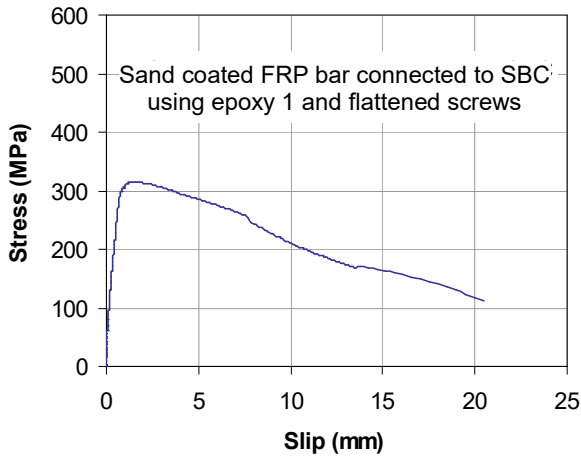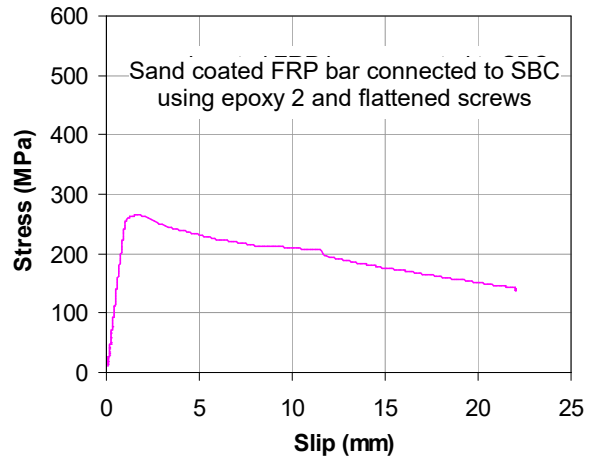

Fig. 16. Sand coated FRP bar connected to SBC using (a) epoxy 1 (Epogrip), and (b) epoxy 2 (Concresive).

Fig. 17. Sand coated FRP bar connected to SBC with flattened screws and epoxy adhesives (a) failure pattern of FRP bar, and (b) inner face of epoxy adhesive inside coupler after pullout of FRP bar.
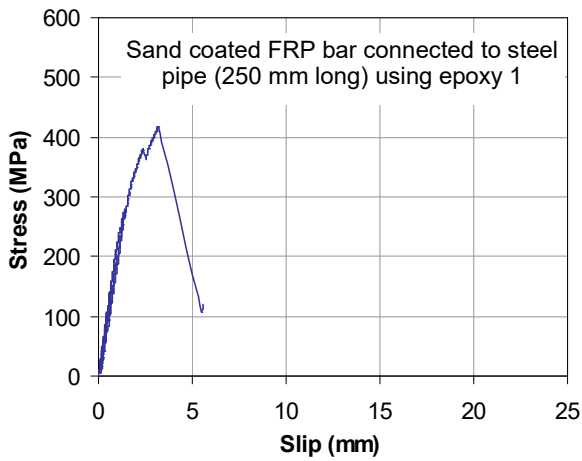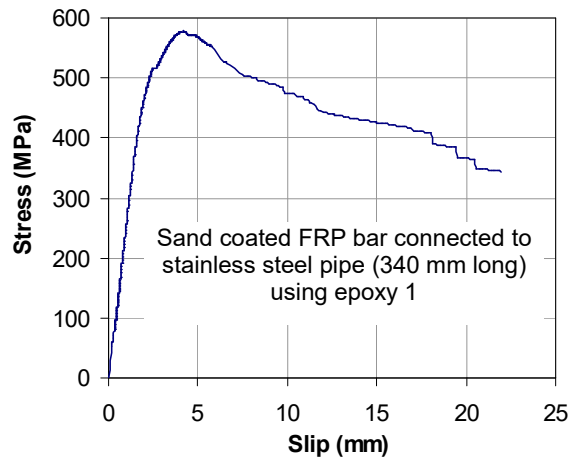
Fig. 18. Sand coated FRP bar connected to SBC with flattened screws and epoxy adhesives of (a) epoxy 1 (Epogrip), and (b) epoxy 2 (Concresive).

Fig. 19. Sand coated FRP bar connected with epoxy 1 (Epogrip) to (a) steel pipe (250 mm long), and (b) stainless steel pipe (340 mm long).

TABLES:

Table 1. Tensile strength test results of steel bars

Bar	Diameter	Yield Strength	Ultimate Strength
	mm	MPa	MPa
Round (smooth)	12.75	338.4	481.7
Deformed (15M)	16.00	524.0	619.5
Deformed (20M)	19.50	440.0	650.0
Deformed (22M)	22.22	503.0	630.0

Table 2. Pullout test results of couplers splicing steel bar

Specimen Name	Bar Diameter	Coupler Type	Yield Load	Bar Slip at $0.5f_y < 0.25$ mm	Ultimate Load	Bar Slip at Ultimate	Failure Pattern*
	mm		kN	mm	kN	mm	
R-1-T1-1	12.75	SBC	43.4	0.076	61.3	20.7	R.R.
R-1-T1-2	12.75	SBC	43.1	0.058	61.0	18.8	R.R.
R-1-T2-1	12.75	DBTC	42.9	0.054	61.1	32.1	R.R.
R-1-T2-2	12.75	DBTC	42.8	0.051	61.2	26.2	R.R.
R-1-T2-3	12.75	DBTC	43.3	0.099	60.5	36.8	R.R.
D-2-T1-1	16.00	SBC	104.2	0.108	122.7	9.1	R.R.
D-2-T1-2	16.00	SBC	103.6	0.098	118.0	12.8	R.R.
D-2-T1-3	16.00	SBC	103.8	0.103	123.9	27.2	R.R.
D-2-T2-1	16.00	DBTC	102.6	0.123	103.6	10.6	C.F.
D-2-T2-2	16.00	DBTC	103.2	0.112	104.6	7.4	C.F.
D-2-T2-3	16.00	DBTC	-	0.092	99.5	5.4	C.F.
D-3-T1-1	19.50	SBC	133.2	0.102	192.3	14.4	R.R.
D-3-T1-2	19.50	SBC	131.7	0.110	195.0	11.0	R.R.

* R.R.: the failure occurred by rupture of the bar, C.F.: the failure occurred at the coupler by pulling the bar splice off.

Table 3. Pullout test results of SMA in SBC coupler (Case 4)

Specimen	f_y	Slip at f_y	ε_{SE}	f_{SE}	Slip at f_{SE}
	MPa	mm	%	MPa	mm
1	401	2.46	6.40	503	10.15
2	409	2.09	6.16	498	9.26
3	405	2.12	6.07	487	9.11
4	389	2.71	6.31	494	11.35